An Examination of the Wrangel Island Sea Ice Thickness Dipole

Spenser Ross and G.W.K. Moore
University of Toronto, Toronto, Ontario, Canada
Contact: Spenser.ross@utoronto.ca

Introduction

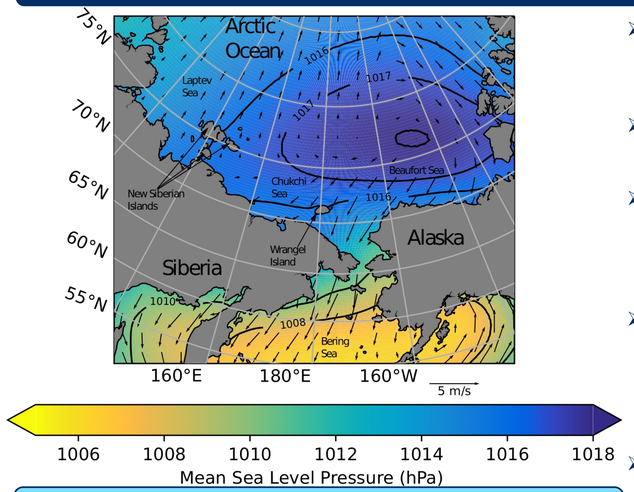

Figure 1. Annual mean sea-level pressure field from the ERA5 reanalysis 1979-2022. Vectors show annual mean ERA5 reanalysis 10m wind over the same period.

- The Beaufort Sea High (BSH) is a high-pressure system located in the Beaufort Sea and influences ocean circulation in the western Arctic known as the Beaufort Gyre.
- Wrangel Island, located in the western Chukchi Sea, typically experiences easterly sea ice motion due to the anticyclonic circulation of the Beaufort Gyre.
- Much of the westward flowing ice is blocked by the island which creates pressure ridges on its eastern side and contributes to the opening of a seasonal polynya to its north-west (Sverdrup, 1929; Cavalieri & Martin, 1994; Moore & Pickart, 2012).
- Wrangel Island's connection to ocean and ice circulation also has an impact on wildlife as it is a critical denning location for Chukchi Sea polar bears and is home to large populations of Pacific walrus, other pinnipeds, and marine mammals (LaRue & Stapleton, 2018; Claudino-Sales, 2019; Hamilton et al., 2022).
- We demonstrate that under climatological BSH conditions, an ice thickness dipole forms across Wrangel Island due to opposing ice divergence and convergence at the island.

Methods

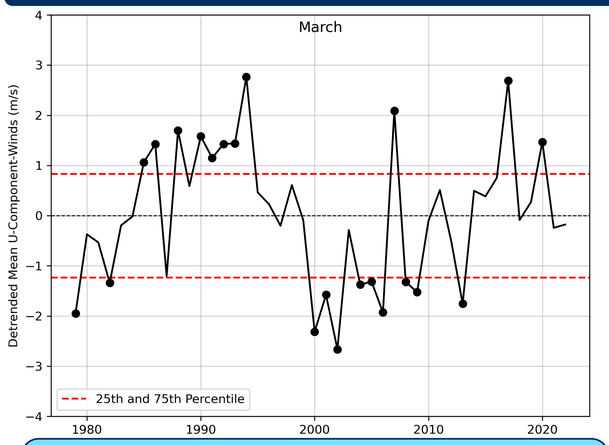

Figure 2. Detrended ERA5 monthly averaged 10m zonal winds (m/s) at Wrangel Island from 1979-2022 for March. The years used in the composites are indicated by black circle markers. The 75th and 25th percentile cut-offs are denoted with a red dashed line.

- For this investigation, we use ERA5 reanalysis monthly mean sea-level pressure and 10m wind data from 1979-2022. We also use PIOMAS ice thickness and ice advection data from 1979-2022.
- The long term trendline was subtracted from mean zonal wind time series at Wrangel Island to create Figure 2, where positive (negative) zonal wind values represent westerly (easterly) winds.
- From the detrended data we determined the top 25% of the years of strongest easterly and westerly monthly mean winds. These years are denoted by black circle markers.
- With these dates, we used monthly averaged ice thickness data to identify composite ice characteristics associated with easterly and westerly winds throughout the year.
- The difference between the composites for the strongest easterly and westerly winds was used to identify the Wrangel Island sea ice dipole (Figure 3).
- The sign of the anomaly in the following fields corresponds to conditions during climatological easterly flow. A reversal in the circulation would result in a flipping of the sign of any anomaly.

Results

- Figure 3 demonstrates the ice thickness dipole in March at Wrangel Island. It shows the difference in monthly mean ice thickness fields between the years of the strongest easterly and westerly winds.
- The difference in mean ice thickness was taken between two polygons on either side of the island (Figure 3) to quantify the dipole's strength. The dipole strength peaks in January at approximately 1m.
- Figure 4 shows the difference in monthly averaged sea-level pressure and 10m wind fields triggering off the same years of strong easterly and westerly winds. There is increased sea-level pressure in the Beaufort Sea extending north toward the Arctic Ocean.
- Thus, months with the strongest easterly winds at Wrangel Island are associated with an increased BSH. This is consistent with the wind vectors flowing clockwise around the region of increased sea-level pressure. This anticyclonic circulation is consistent with the climatological Beaufort Gyre and forces easterly winds at Wrangel Island.
- Figure 5 shows the difference in the monthly mean change in ice thickness due to advection between years of strong easterly and westerly winds. There is an increase in ice thickness due to advection to the east of the island and a decrease to the west of the island. Thus, strong easterly winds at the island are associated with ice advected towards the island from the east and advected away from the island towards the west.

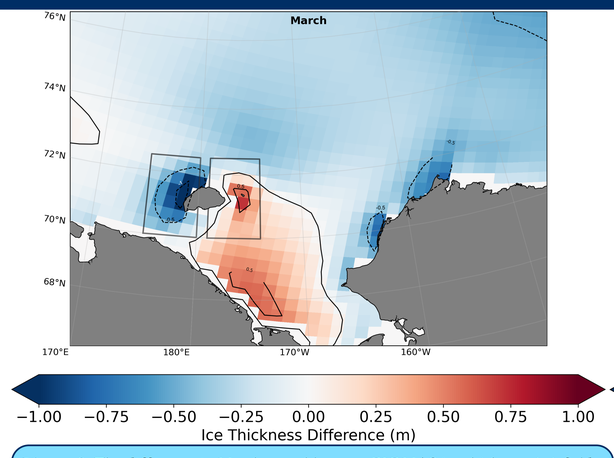

Figure 3. The difference in March monthly mean PIOMAS ice thickness (m) fields between years of strong easterly and westerly winds. The coordinates bounding the west polygon are 70N to 72.5N and 175E to 180. The coordinates bounding the east polygon are 70N to 72.5N and 174W to 179W.

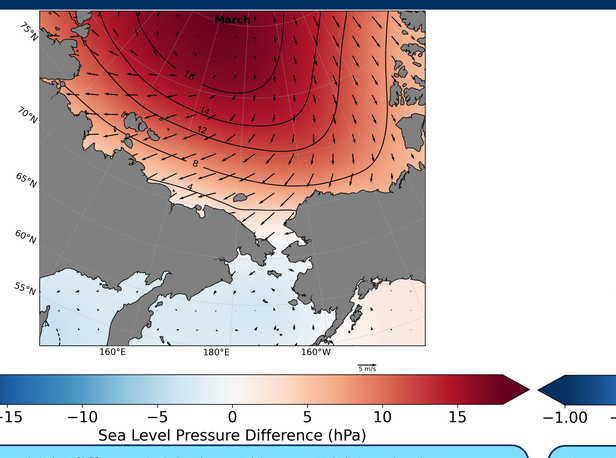

Figure 4. The difference in March monthly mean ERA5 sea-level pressure (hPa) fields between years of strong easterly and westerly winds at Wrangel Island. The difference in ERA5 wind vectors (m/s) is also shown.

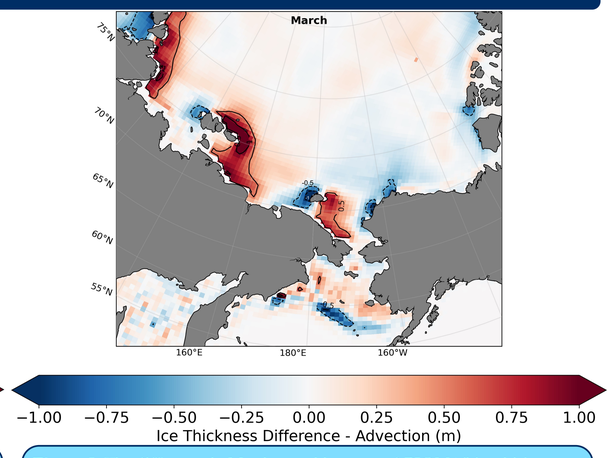

Figure 5. The difference in March monthly averaged PIOMAS ice thickness (m) due to ice advection between years of strong easterly and westerly winds at Wrangel Island.

Conclusions

- The climatological BSH and Beaufort Gyre conditions force easterly surface winds and sea ice towards Wrangel Island.
- Much of this ice is blocked by the island, creating a region of increased ice thickness and pressure ridges to the east of the island and a region of decreased ice thickness to the west of the island. The sense of the dipole is reversed under westerly flow.
- Similar signals are found throughout the western Arctic, for instance, across the New Siberian Islands, which can be seen in the ice thickness anomalies due to ice advection in Figure 5.
- We find that strong easterly winds and the sea ice thickness dipole at Wrangel Island are associated with an increased BSH. Accordingly, the dipole is found to be linked to increased anticyclonic wind and ice motion in the region which is consistent with the circulation of the climatological Beaufort Gyre forcing easterly ice motion near Wrangel Island.
- During these typical conditions, we find the dipole is associated with increased ice advection towards the island from the East and away from the island towards the West. The opposite is true during reversals of the Beaufort Gyre caused by collapses in the BSH.
- Future BSH collapses and other Arctic climate changes, such as thinning sea ice, will have impacts on the formation of the sea ice thickness dipole at Wrangel Island.
- Future work must examine the extent to which changes to the sea ice thickness dipole can impact the formation of the Wrangel Island polynya, and the food availability of polar bears and Pacific walrus who live on the island.

References

Cavalieri, D. J., & Martin, S. (1994). The contribution of Alaskan, Siberian, and Canadian coastal polynyas to the cold halocline layer of the Arctic Ocean. Journal of Geophysical Research, 99(C9), 18343. doi: 10.1029/94JC01169

Claudino-Sales, V. (2019). Natural System of Wrangel Island Reserve, Russia. In Coastal World Heritage Sites (Vol. 28, pp. 209–214). Dordrecht: Springer Netherlands. doi: 10.1007/978-94-024-1528-5 31

Copernicus Climate Change Service. (2019). ERA5 monthly averaged data on single levels from 1979 to present [dataset]. ECMWF. doi: 10.24381/CDS .F17050D7

Hamilton, C. D., Lydersen, C., Aars, J., Acquarone, M., Atwood, T., Baylis, A., . . . Kovacs, K. M. (2022, December). Marine mammal hotspots across the circumpolar Arctic. Diversity and Distributions, 28(12), 2729–2753. doi: 10.1111/ddi.13543

LaRue, M. A., & Stapleton, S. (2018, December). Estimating the abundance of polar bears on Wrangel Island during late summer using high-resolution satellite imagery: a pilot study. Polar Biology, 41(12), 2621–2626. doi: 10.1007/s00300-018-2384-4

Moore, G., & Pickart, R. S. (2012, March). The Wrangel Island Polynya in early summer: Trends and relationships to other polynyas and the Beaufort Sea High: The Early Summer Wrangel Island Polynya. Geophysical Research Letters, 39(5), n/a–n/a. doi: 10.1029/2011GL050691

Sverdrup, H. U. (1929). The waters on the North-Siberian Shelf (Vol. 4) (No. 2). Geofysisk Institutt, Bergen.

Zhang, J., & Rothrock, D. A. (2003, May). Modeling Global Sea Ice with a Thick- ness and Enthalpy Distribution Model in Generalized Curvilinear Coordinates. Monthly Weather Review, 131(5), 845–861. doi: 10.1175/1520-0493(2003)131⟨0845:MGSIWA⟩2.0.CO;2